# A Novel Ultra-Wideband Circular Slot Antenna Excited with a Dipole Element

Mario Leib, Michael Frei, and Wolfgang Menzel

University of Ulm, Microwave Techniques, Albert-Einstein-Allee 41, 89081 Ulm, Germany
Email: mario.leib@uni-ulm.de

***Abstract*—In this contribution, a novel differentially-fed planar ultra-wideband antenna is presented and discussed in detail. This antenna is intended to operate in the FCC frequency range from 3.1 GHz to 10.6 GHz. It is composed of a circular aperture in ground plane and a broadband dipole element exciting the slot aperture. This combination leads to an outstanding radiation performance with a quite uniform radiation pattern over frequency and a mean gain of 2.9 dBi. The measured return loss of the realized antenna is better than 10 dB from 3.9 GHz to 9.8 GHz including an inevitable balun for characterization, and without the balun the 10 dB bandwidth is extended to 3.4 GHz–11 GHz according to the simulation results. Besides the characterization of the antenna in frequency domain, the time domain behavior is shown and demonstrates the antenna's capability for impulse based UWB radio.**

***Index Terms*—circular slot antenna, ultra-wideband (UWB), differential feeding, planar, dipole antenna**

## I. Introduction

Antennas with broadband performance are of interest in various areas, e. g. as reference antennas in measurement chambers [1], in ground penetrating radars for landmine detection [2], and in many military systems [3]. Ultra-wideband antennas (UWB) are defined by a fractional bandwidth of ≥20% or a bandwidth of at least 500 MHz [4]. The recent trend for the design of UWB antennas between 3.1 GHz and 10.6 GHz is pushed by the decision of the FCC to give a generic admission for the use of UWB systems in this frequency range. Since this decision in 2002, mainly civilian applications are in the focus of research activities. Short-range, high data-rate links for consumer electronics, breast cancer detection and patient monitoring in the medical environment [5], [6] or the detection of trapped people [7] are just some examples. The requirements for UWB antennas are a return loss of ≥10 dB, a constant radiation pattern over frequency, and a low dispersive behavior, in particular for impulse based UWB systems. Planar antennas are favored resulting in compact UWB communication or radar front-ends.

The demanded ultra-wideband impedance matching behavior can be achieved using planar monopole antennas with rectangular, elliptical or more complex shapes [8]. Due to the compact size and therefore reduced ground plane of these monopole antennas, parasitic leakage waves exist and propagate along the outer surface of the coaxial shell of the feeding cable [9]. These cable currents cause an undesired distortion of the radiation pattern. In [10] and [11] the insertion of blocking slots in the ground plane is proposed as a suitable countermeasure. However, this method just reduces the cable current effect and does not provide a complete suppression. Differentially fed antennas are resistant to cable currents due to the virtual ground plane. In addition, symmetrical feeding structures radiate less, and they are preferred in combination with differential monolithic integrated circuits (MMICs) because no baluns are needed. Baluns realized either in a passive or active manner lead to increased insertion loss and/or additional power consumption. The benefits of differential MMICs itself are less susceptibility to interferences due to common-mode rejection, a better tolerance for poor RF grounds, improved power supply rejection, and immunity to power supply noise.

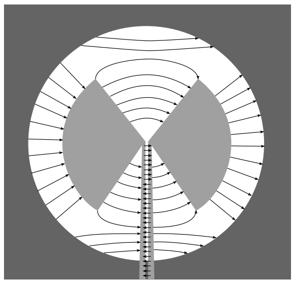

Fig. 1. Typical E-field distribution in the antenna slot.

Balanced UWB antennas in planar technique are typically realized by fat dipoles with dipole shapes similar to UWB monopoles. For instance, a circular shape is applied in [12], and if fed by a coplanar stripline, the main beam of the antenna splits into two beams above 6 GHz reducing the radiation performance for high frequencies. The effect is caused by the fact that the antenna acts like a tapered slot antenna with increasing frequency, which is a general disadvantage for this kind of antennas.

In this publication, a novel approach is applied in order to obtain a symmetrical UWB antenna with uniplanar feeding. A broadband slot antenna with a circular aperture is excited with a planar dipole element (see Fig. 1). The method is similar to [13], where a three-dimensional dipole element is used to excite a dielectric rod in order to achieve a directional UWB antenna. As will be shown, the combination of slot and dipole element leads to a compact planar antenna with a steady radiation characteristic over frequency.

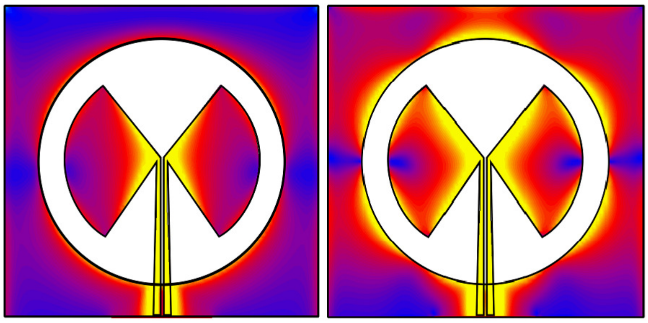

Fig. 2. Simulated surface currents for 6.85 GHz (left) and 9.8 GHz (right).

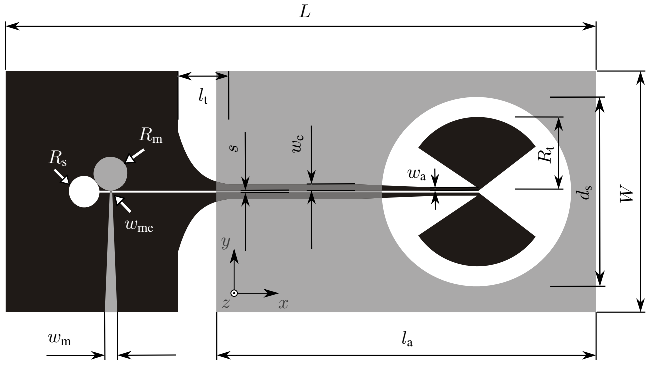


Fig. 3. Sketch of the antenna layout including balun and all geometrical parameters.

TABLE I
DIMENSIONS OF THE ANTENNA AND THE BALUN ACCORDING TO FIG. 3.

| $L$ | $W$ | $R_m$ | $R_s$ | $R_t$ | $d_s$ |
|---|---|---|---|---|---|
| 92.52 mm | 37.8 mm | 2.4 mm | 2.8 mm | 11.31 mm | 29.68 mm |

| $l_a$ | $l_t$ | $s$ | $w_a$ | $w_c$ | $w_m$ | $w_{me}$ |
|---|---|---|---|---|---|---|
| 59.62 mm | 8 mm | 0.3 mm | 0.48 mm | 1 mm | 1.86 mm | 0.4 mm |

## II. Antenna Design

### A. Radiating Element

The basic concept of the antenna is the broadband excitation of a circular slot antenna. Instead of a microstrip line ending in an open stub, like in [14], a differential feeding with a coplanar stripline is chosen. Each transmission line of the coplanar stripline ends in an open stub (see Fig. 1). The length of a stub is $\lambda/4$ at the center frequency of 6.85 GHz and the shape is a segment of a circle. The angle of the circle segment is critical for the broadband operation of the antenna. If not chosen properly, the antenna behaves like a tapered slot antenna and mainly radiates along the slot defined by the two stub sides. In our case an angle of 110° is found to be an appropriate value. From a different point of view, this stub configuration can also be seen as a broadband $\lambda/2$ dipole antenna exciting the electrical field in the slot as sketched in Fig. 1.

The circumference of the slot aperture is chosen to be two times the wavelength at the center frequency. Hence, two wavelengths equals the circumference at 6.85 GHz leading to a resonance. In an analogous manner, one and three wavelengths fit on the slot outline for 0.5 and 1.5 times the center frequency. The excitation of these two resonances is caused by the broadband operation of the dipole element. This behavior of the antenna is visualized in Fig. 2, where the surface currents on the antenna are shown. There, the two and three wavelengths around the slot can be clearly identified for 6.85 GHz and 9.8 GHz, respectively. The three resonances can be also seen in the return loss of the antenna (compare Fig. 5, antenna without balun).

The antenna is designed for the substrate material RO4003 ($\varepsilon_r = 3.38$) with a height of 0.81 mm. All antenna parameters are optimized for operation in the FCC frequency band using Microwave Studio [15]. The obtained dimensions are listed in Table I. The impedance of the coplanar microstrip lines is 144 Ω without and 134 Ω with a ground plane on the backside. A taper is applied to transform the impedance to 100 Ω in order to be compatible with differential ICs.

### B. Balun

Albeit no balun is needed in combination with differential ICs, a balun is mandatory in order to characterize the antenna with standard single-ended measurement equipment. A passive UWB balun is designed for the applied substrate material, and the balun layout is displayed in Fig. 3 together with the radiating element. The balun structure can be divided into two parts. The first part is a broadband transition from a 50 Ω microstrip line to a slot line, whereas circular-shaped stubs are applied according to [16]. In the second part, the slot line is transformed into a coplanar strip line with 100 Ω impedance using an exponential taper. The combination of these two transitions results in ultra-wideband performance as shown in [17]. The dimensions of this balun are also summarized in Table I.

## III. Realized Antenna

In Fig. 4 the manufactured planar antenna is displayed comprising the balun and a housing. The housing, made of

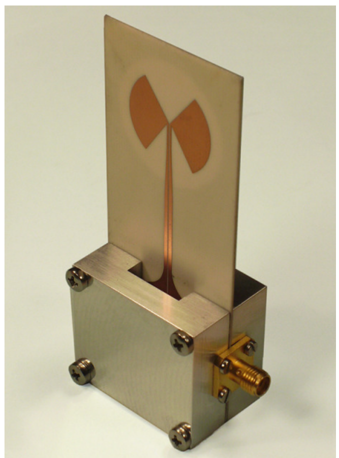

Fig. 4. Photograph of the manufactured antenna with housing.

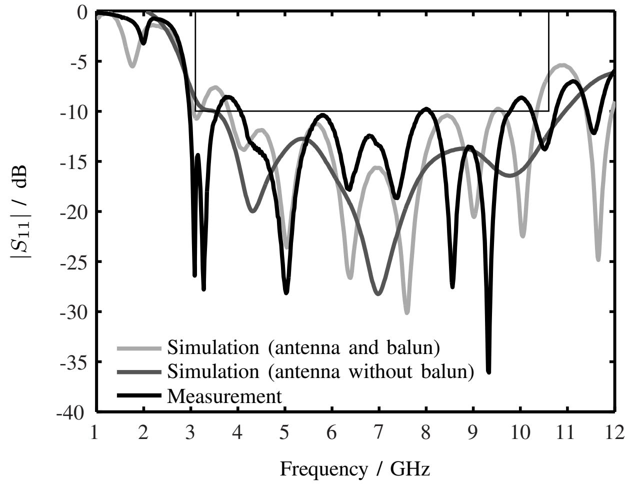


Fig. 5. Simulated and measured matching performance of the antenna.

aluminum and filled with absorber sheets, is mandatory in order to shield the parasitic radiation of the balun. Without a shielding around the balun the measured radiation pattern would be distorted significantly. Furthermore, the housing acts as a mount and is used to fix the SMA connector.

## IV. Antenna Characterization

### A. *Frequency Domain*

As can be seen in Fig. 5, the measured and simulated return loss of the overall antenna structure agree quite well, although the housing is not included in the simulation. The return loss criterion of 10 dB is achieved from 3.9 GHz to 9.8 GHz and therewith does not comply with the FCC frequency band completely. However, if the antenna is operated differentially, that means without balun, even a higher bandwidth is possible as indicated by the simulation of the return loss of solely the radiating element.

The simulated and measured radiation pattern of the antenna for the E-plane ($y$-$z$-plane) and the H-plane ($x$-$z$-plane) were normalized to the maximum gain and are displayed in Fig. 6 and Fig. 7, respectively. Due to the suppression of the undesired radiation by the balun, a good agreement between simulation and measurement is achieved. The given diagrams only show the radiation pattern in forward direction (negative $z$-direction, see Fig. 3), but the radiation characteristic in backward direction (positive $z$-direction) is identical. Remarkable is the steady behavior of the radiation pattern over frequency in both planes without any side lobes, which is caused by the interaction of dipole element and slot. Such a performance has neither be obtained by a UWB dipole [12] nor by monopole

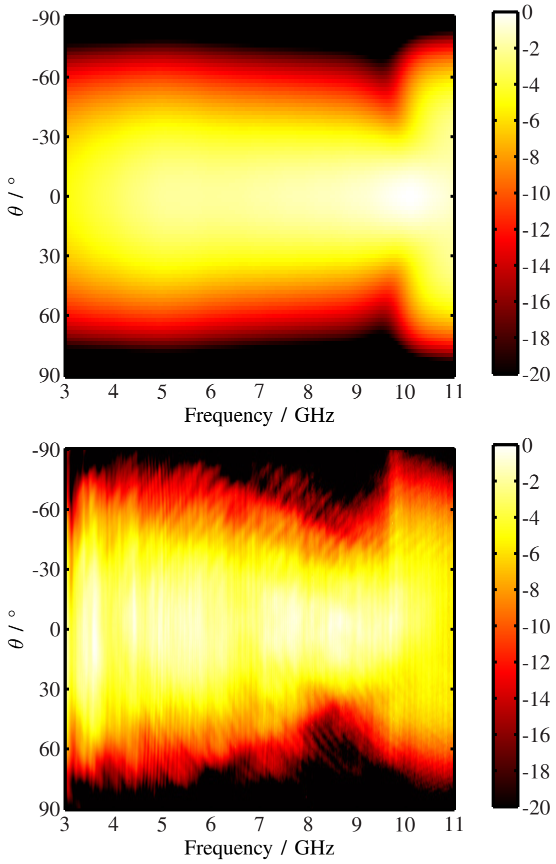


Fig. 6. Simulated (top) and measured (bottom) normalized radiation diagram for the E-plane in dB.

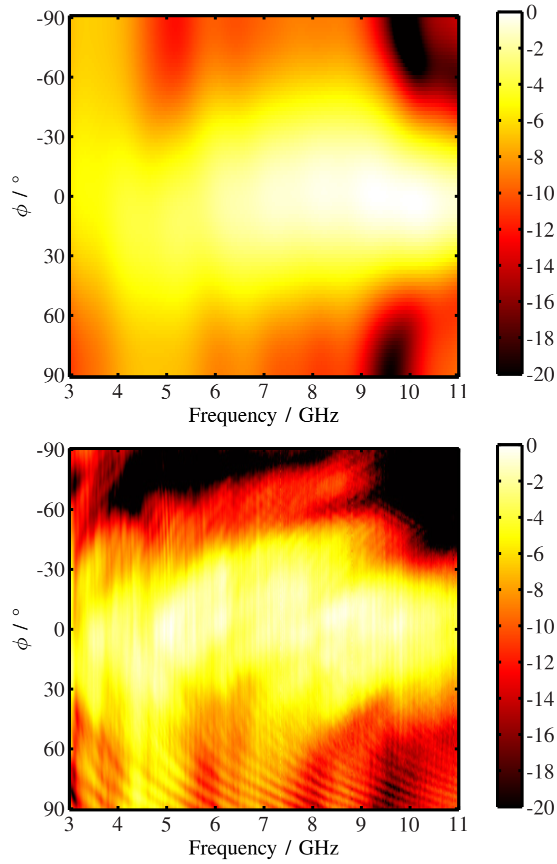


Fig. 7. Simulated (top) and measured (bottom) normalized radiation diagram for the H-plane in dB.

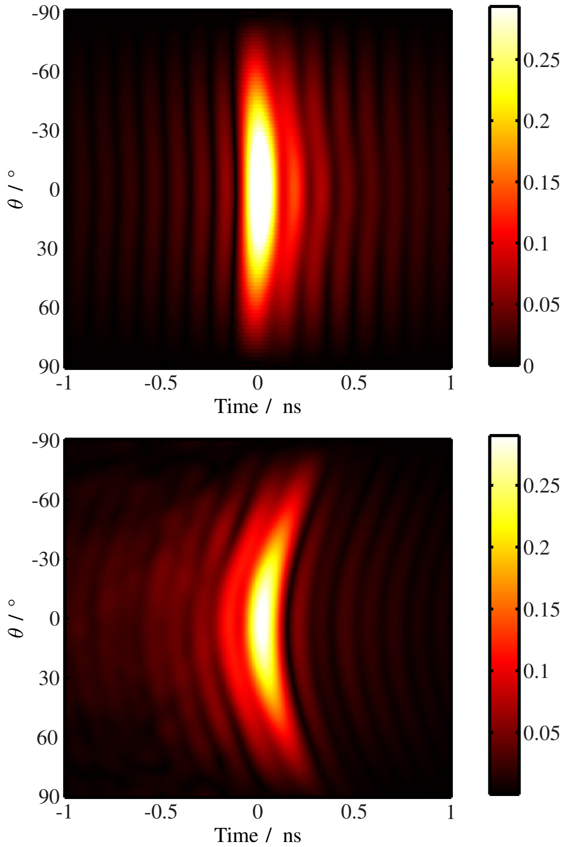


Fig. 8. Simulated (top) and measured (bottom) impulse response envelope for the E-plane in $\frac{\mathrm{m}}{\mathrm{ns}}$.

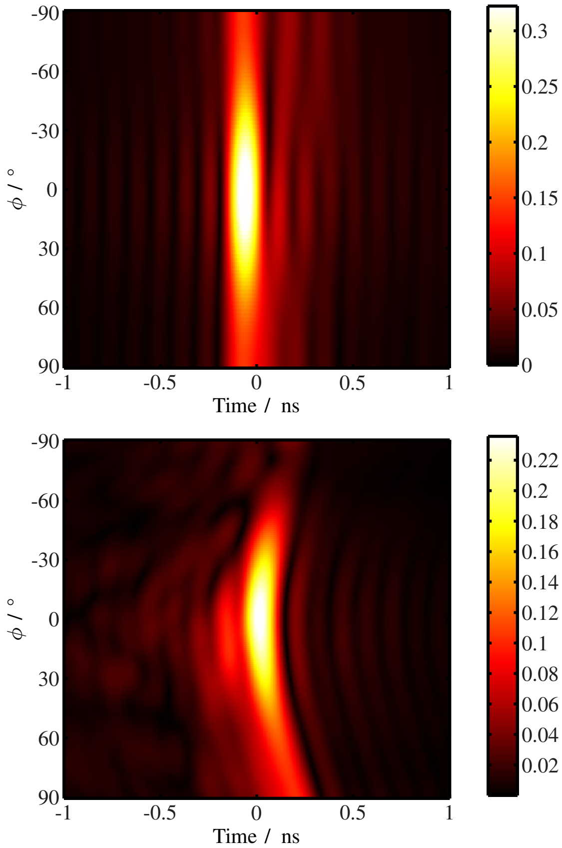


Fig. 9. Simulated (top) and measured (bottom) impulse response envelope for the H-plane in $\frac{\mathrm{m}}{\mathrm{ns}}$.

antennas [14].

The slight asymmetry in the H-plane of the radiation pattern is caused by the asymmetrical geometry of the antenna due to the feeding structure; this is observable in both simulation and measurement. Shadowing effects produced by the housing are the reason for the lower radiation at rotation angles around $-90°$ in the H-plane measurement. The mean gain of the antenna is 2.9 dBi in the frequency range 3 GHz–11 GHz determined by the measurement results, whereas the maximum gain is 5 dBi. The antenna is linearly polarized with a mean cross-polarization rejection better than 15 dB.

## *B. Time Domain*

Antennas with a low dispersive behavior are required for impulse based UWB radio, corresponding to a linear phase or a constant group delay in the frequency domain. Alternatively, the time domain characteristic can be analyzed in order to evaluate the antenna behavior. The envelope of the impulse response obtained with the simulated and measured data using the Fourier transformation according to [18] are shown in Fig. 8 and Fig. 9 for both planes. The difference in the shape of the impulse response between measurement and simulation arises form the fact that the antenna phase center is not positioned at the rotation axis during the measurement.

The simulated and measured impulse response in the main radiation direction are directly compared in Fig. 10. Albeit the characteristic of the used UWB reference antenna (a ridge waveguide horn antenna) is not corrected, a similar response is obtained. The figure of merit for the dispersive behavior is the full width at half maximum (FWHM) of the impulse response

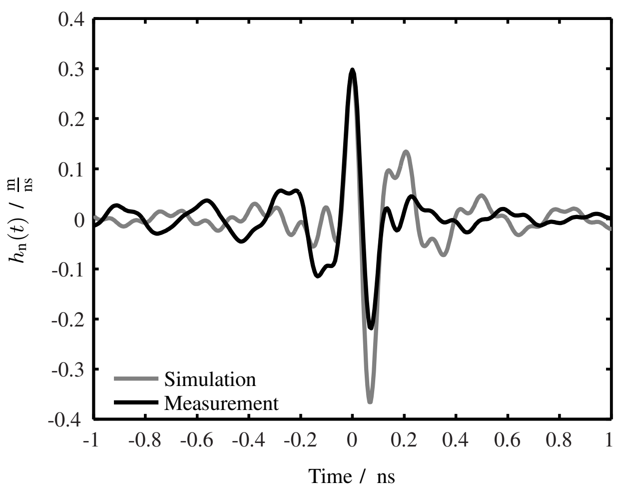


Fig. 10. Simulated and measured impulse response of the antenna in main radiation direction ($\theta = \phi = 0°$).

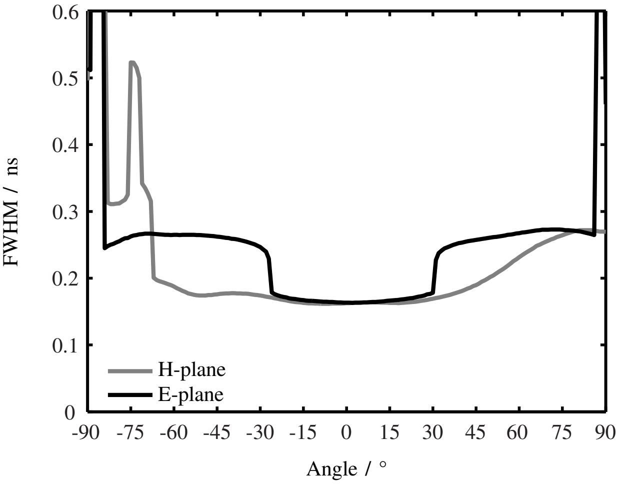


Fig. 11. Full width at half maximum (FWHM) of the measured impulse response as function of the radiation angle (E- and H-plane).

envelope shown in Fig. 11 for all rotation angles. Within the main beam the FWHM is quite constant with a value of 190 ps making this antenna suitable for impulse based systems.

## V. Conclusion

The described UWB planar slot antenna is compact with its dimension of 4 cm $\times$ 4 cm considering only the radiating element. The main benefit compared to other single-ended and differential planar antennas is the very uniform radiation characteristic over frequency, leading also to a good time domain behavior. This performance makes the antenna very attractive for all kind of UWB systems, where small front-ends are desired and, in particular, if differential MMICs are used.

## Acknowledgment

This work has been funded by the German Research Foundation (DFG) under the program UKoLoS.

## References

[1] V. Rodriguez, "A multi-octave, open-boundary, quad-ridge horn antenna for use in the S- to Ku-bands," *Microwave Journal*, vol. 49, no. 3, p. 83, Mar. 2006.

[2] G. Stickley, I. Longstaff, and M. Radcliffe, "Synthetic aperture radar for the detection of shallow buried objects," in *EUREL International Conference on the Detection of Abandoned Land Mines*, no. 431, Oct. 1996, pp. 160–163.

[3] J. D. Taylor, Ed., *Ultra-wideband radar technology*. Boca Raton: CRC Press, 2001.

[4] Federal Communications Commission, "Revision of part 15 of the commission's rules regarding ultra-wideband transmission systems," FCC, Washington D.C., USA, First Report & Order 48-02, Apr. 2002.

[5] X. Li, E. J. Bond, B. D. V. Veen, and S. C. Hagness, "An overview of ultra-wideband microwave imaging via space-time beamforming for early-stage breast-cancer detection," *IEEE Transactions on Antennas and Propagation*, vol. 47, no. 1, pp. 19–34, Feb. 2005.

[6] M. Leib, E. Schmitt, A. Gronau, J. Dederer, B. Schleicher, H. Schumacher, and W. Menzel, "A compact ultra-wideband radar for medical applications," *Frequenz*, vol. 63, no. 1-2, pp. 1–8, Feb. 2009.

[7] A. Yarovoy, L. Ligthart, J. Matuzas, and B. Levitas, "UWB radar for human being detection," *IEEE Aerospace and Electronic Systems Magazine*, vol. 21, no. 11, pp. 22–26, Nov. 2006.

[8] Z. N. Chen, M. J. Ammann, X. Qing, X. H.Wu, T. S. See, and A. Cai, "Planar antennas," *IEEE Microwave Magazine*, vol. 7, no. 6, pp. 63–73, Dec. 2006.

[9] T. Hertel, "Cable-current effects of miniature UWB antennas," in *IEEE International Symposium on Antennas and Propagation*, vol. 3A, Jul. 2005, pp. 524–527.

[10] Z. N. Chen, T. S. See, and X. Qing, "Small printed ultrawideband antenna with reduced ground plane effect," *IEEE Transactions on Microwave Theory and Techniques*, vol. 55, no. 2, pp. 383–388, Feb. 2007.

[11] D.-H. Kwon and Y. Kim, "Suppression of cable leakage current for edge-fed printed dipole UWB antennas using leakage-blocking slots," *IEEE Antennas and Wireless Propagation Letters*, vol. 5, no. 1, pp. 183–186, Dec. 2006.

[12] A. V. Vorobyov, S. Bagga, A. G. Yarovoy, S. A. P. Haddad, W. A. Serdijn, J. R. Long, Z. Irahhauten, and L. P. Ligthart, "Integration of a pulse generator on chip into a compact ultrawideband antenna," *IEEE Transactions on Antennas and Propagation*, vol. 56, no. 3, pp. 858–868, Mar. 2008.

[13] M. D. Blech and T. F. Eibert, "A dipole excited ultrawideband dielectric rod antenna with reflector," *IEEE Transactions on Antennas and Propagation*, vol. 55, no. 7, pp. 1948–1954, Jul. 2007.

[14] E. S. Angelopoulos, A. Z. Anastopoulos, D. I. Kaklamani, A. A. Alexandridis, F. Lazarakis, and K. Dangakis, "Circular and elliptical cpw-fed slot and microstrip-fed antennas for ultrawideband applications," *IEEE Antennas and Wireless Propagation Letters*, vol. 5, no. 1, pp. 294–297, Dec. 2006.

[15] *Microwave Studio*, CST - Computer Simulation Technology, Version 2008.

[16] B. Schueppert, "Microstrip/slotline transitions: Modeling and experimental investigation," *IEEE Transactions on Microwave Theory and Techniques*, vol. 36, no. 8, pp. 1272–1282, Aug. 1988.

[17] M. Frei, M. Leib, and W. Menzel, "A symmetrically fed aperture-coupled stacked-patch antenna," acccepted for IEEE International Symposium on Antennas and Propagation, Jul. 2009.

[18] W. Sörgel and W. Wiesbeck, "Influence of the antennas on the ultra-wideband transmission," *EURASIP Journal on Applied Signal Processing*, vol. 2005, no. 3, pp. 296–305, 2005.